Stochastic Acceleration of ^{3}He and ^{4}He by Parallel Propagating Plasma Waves

Siming Liu[1], Vahé Petrosian[1,2], and Glenn M. Mason[3]

ABSTRACT

Stochastic acceleration of ^{3}He and ^{4}He from a thermal background by parallel propagating turbulent plasma waves with a single power-law spectrum of the wavenumber is studied. In the model, both ions interact with several resonant modes. When one of these modes dominates, the acceleration rate is reduced considerably. At low energies, this happens for ^{4}He, but not for ^{3}He where contributions from the two stronger modes are comparable so that acceleration of ^{3}He is very efficient. As a result, the acceleration of ^{4}He is suppressed by a barrier below ~ 100 keV nucleon^{-1} and there is a prominent quasi-thermal component in the ^{4}He spectra, while almost all the injected ^{3}He ions are accelerated to high energies. This accounts for the large enrichment of ^{3}He at high energies observed in impulsive solar energetic particle events. With reasonable plasma parameters this also provides a good fit to the spectra of both ions. Beyond ~ 1 MeV nucleon^{-1}, the spectrum of ^{3}He is softer than that of ^{4}He, which is consistent with the observed decrease of the ^{3}He to ^{4}He ratio with energy. This study also indicates that the acceleration, Coulomb losses and diffusive escape of the particles from the acceleration site *all* play important roles in shaping the ion spectra. This can explain the varied spectral shapes observed recently by the *Advanced Composition Explorer*.

Subject headings: acceleration of particles — plasma — Sun: abundances — Sun: flares — turbulence

[1]Center for Space Science and Astrophysics, Department of Physics, Stanford University, Stanford, CA 94305; liusm@stanford.edu

[2]Department of Physics and Applied Physics, Stanford University, Stanford, CA 94305; vahe@astronomy.stanford.edu

[3]Department of Physics and Institute for Physical Sciences and Technology, University of Maryland, College Park, MD 20742-4111; glenn.mason@umail.umd.edu

1. Introduction

The abundance and spectra of most ions observed in impulsive solar energetic particle events (SEPs) qualitatively agree with predictions of stochastic acceleration (SA) by plasma waves or turbulence (PWT) (e.g. Möbius et al. 1980; 1982). However, the observed enrichment of ^{3}He, sometimes by more than four orders of magnitude over its coronal abundance (Hsieh & Simpson 1970; Serlemitsos & Balasubrahmanyan 1975; Mason et al. 2002), remains a theoretical challenge. The aim of this paper is to provide an explanation for this observation in the frame of SA models.

Solar ^{3}He rich events are enriched also in other heavy elements (Hurford et al. 1975; Mason et al. 1986) and are closely related to impulsive X-ray flares, scatter-free electron events, and type III radio bursts (Reames, von Rosenvinge & Lin 1985; Reames, Meyer & von Rosenvinge 1994; Mazur, Mason & Klecker 1995; Mason et al. 2002), indicating that a common particle acceleration process may be responsible for all these features. Among the acceleration mechanisms applied to solar flares, the theory of SA, a second order Fermi acceleration process by PWT, has achieved several significant successes. The theory was first introduced to account for the acceleration of protons and other ions responsible for the observed nuclear gamma ray line emissions (Ramaty 1979; Hua, Ramaty & Lingenfelter 1989). Later it was shown that it is also applicable to the acceleration of electrons, which produce the impulsive hard X-ray emission (Miller & Ramaty 1987; Hamilton & Petrosian 1992; Park, Petrosian & Schwartz 1997; Petrosian & Donaghy 1999). A recent study of SA by cascading Alfvén turbulence indicated that it may also explain heavy ion acceleration as well (Miller 2003).

It is generally accepted that the enrichment of ^{3}He is related to its peculiar charge to mass ratio so that certain plasma waves resonantly accelerate or heat it to high energies, producing the observed abundance ratio at a few MeV nucleon^{-1} (Möbius et al. 1980; Zhang 1999). Previous work either discusses the feasibility of selective accelerating ^{3}He from very low energies (Temerin & Roth 1992; Miller & Viñas 1993), or considers a two-stage mechanism; a selective preheating process followed by an acceleration applicable to all ions (Fisk 1978). The former cannot be compared with observation directly because the acceleration of other ions has not been addressed accordingly. For the latter, the observed abundance pattern at high energies is determined by the preheating processes (Paesold, Kartavykh & Benz 2003) and the predicted spectrum depends on several parameters with the corresponding physical processes unspecified (Sakurai 1974; Zhang 1995).

Given its simple dispersion relation, Alfvén turbulence is used in most of the SA models (Ramaty 1979; Möbius et al. 1982), which cannot explain the varied ion spectral forms and underestimates the production rate of higher energy particles in disagreement with the recent

observations by the *Advanced Composition Explorer* (*ACE*; Mason et al. 2002). However, low energy particles mostly interact with cyclotron and/or whistler waves. To understand the acceleration of particles from a thermal background, it is necessary to use the exact dispersion relation (Steinacker et al. 1997). We have carried out such an investigation recently, which addresses the acceleration of electrons vs protons by waves propagating parallel to magnetic field lines (Petrosian & Liu 04, PL04 for short). Besides its achievements in explaining many features of solar flares, we found that the acceleration of low energy protons can be suppressed significantly relative to the electron acceleration due to the dominance of the wave-proton interaction by the resonant Alfvén mode.

In this letter, we show that a similar mechanism makes the acceleration of low energy ^{3}He much more favorable relative to that of ^{4}He. Because their loss rates are comparable, such a mechanism basically depletes ^{3}He from the thermal background to $\sim$ MeV energies while most of the ^{4}He ions are "trapped" at low energies, resulting a prominent quasi-thermal ^{4}He component. The model not only explains the enrichment of ^{3}He at a few MeV nucleon^{-1}, but also accounts for the flattening of the ^{3}He spectrum at lower energies (Mason, Dwyer & Mazur 2000; Mason et al. 2002). It also predicts that beyond a few MeV nucleon^{-1} the spectrum of ^{4}He is always harder than the ^{3}He spectrum. In the next section, we present our SA model. Its application to SEPs is discussed in § 3. In § 4, we summarize our results and discuss their implications.

2. Stochastic Ion Acceleration

The theory of SA by parallel propagating waves is explored in detail in PL04. Here, we highlight a few key points, which are crucial in understanding the ion acceleration process.

First, a magnetized plasma can be characterized by the ratio of the electron plasma frequency $\omega_{\rm pe}$ to gyrofrequency $\Omega_{\rm e}$:

$$\alpha = \omega_{\rm pe}/\Omega_{\rm e} = 3.2(n_{\rm e}/10^{10}{\rm cm}^{-3})^{1/2}(B_0/100~{\rm G})^{-1}\,, \tag{1}$$

where $n_{\rm e}$ is the electron number density and B_0 is the large scale magnetic field. To describe the wave modes in the plasma, one also needs to know the abundance of ions. In our case, the inclusion of α-particle, whose number density is about 10% of the proton density, is essential while other heavier elements have little effect on the dispersion relation $\omega = \omega(k)$ (Steinacker et al. 1997), where ω is the wave frequency and k is the wavenumber.

Low energy ions mostly interact with left-handed polarized waves. Figure 1 shows the dispersion relation of these wave modes as indicated by the dotted curves in a plasma with

$\alpha = 0.45$ and $Y_{He} = 0.08$, where Y_{He} is the abundance of α-particle (here following the notation in PL04, negative frequencies indicate that the waves are left-handed polarized). There are two distinct branches, which we call ^{4}He-cyclotron branch (HeC: upper one) and proton-cyclotron branch (PC: lower one) because they asymptotically approach the corresponding ion cyclotron waves at large wavenumbers. At small k, HeC branch gives the Alfvén waves, while the PC branch approaches a wave frequency $\omega_{PC} \simeq (1/2 + Y_{He})\Omega_p$, where Ω_p is the proton gyrofrequency.

The acceleration process is determined by the resonant wave-particle interaction. The waves and particles couple strongly when the resonant condition $\omega = k\beta c\mu - \Omega_i\gamma^{-1}$, is satisfied, where βc, μ, Ω_i, and γ are respectively the velocity, the pitch angle cosine, the nonrelativistic gyrofrequency, and the Lorentz factor of the ions. Figure 1 also shows this resonant condition (straight lines) for ^{3}He and ^{4}He with $\mu = 1$ and two values of energy: $E = 0.5$ and 47 keV per nucleon. The intersection points of these lines with the dotted curves for the dispersion relation satisfy the resonant condition and indicate strong wave-particle couplings. The wave-particle interaction rates are calculated by adding contributions from these points (PL04).

At low energies (e.g. $E = 0.5$ keV nucleon^{-1} in the figure) ^{4}He interacts only with two waves, one from the HeC and one from PC (not shown in the figure because of its large wavenumber). On the other hand, ^{3}He can interact with four waves, three of them from the PC branch (two of them are shown in the figure) and one from the HeC branch (also not shown in the figure)[1]. As shown in Figure 1 there are two resonant modes for ^{3}He with nearly equal and small wavenumbers while ^{4}He has one resonant mode at low k (see circles in Fig. 1); the next important resonant mode of ^{4}He is at much larger k value beyond the range of the figure. Consequently, for a power law spectrum of turbulence, the interaction of low energy ^{4}He will be dominated by a single mode from the HeC branch, giving rise to a very low acceleration rate relative to ^{3}He (see discussion below)[2]. This is not true for particles with high energies ($E = 47$ keV nucleon^{-1} in the figure). For these particles, the two stronger resonant modes have comparable contributions for both ions.

Following previous studies (Dung & Petrosian 1994; PL04), we will assume that the turbulence has a power law spectrum $\mathcal{E}(k) \propto k^{-q}$ with a low wavenumber cutoff k_{min}, which

---

[1]Both ions also interact with a right-handed polarized wave in the electron cyclotron branch. Because its contribution to the interaction rates of low energy ions is small, we do not discuss this branch here. However, the contribution of this wave branch is included in the numerical calculation below.

[2]It should be noted that this in not true for ions with nearly 90° pitch angle ($\mu \ll 1$). However, this contributes little to the acceleration as a whole because there are few such particles

corresponds to the turbulence generation scale and determines the maximum energy of the accelerated particles. For a turbulence spectral index $q \leq 1$, a high wavenumber cutoff is also required to ensure the convergence of the total turbulence energy density. In this case, we choose k_{max} large enough so that the acceleration of particles from the thermal background is not affected by this cutoff. Then the characteristic interaction time scale τ_{p} is given by

$$\tau_{\mathrm{p}}^{-1} = \frac{\pi}{2}\Omega_{\mathrm{e}} \left[\frac{\mathcal{E}_{\mathrm{tot}}}{B_0^2/8\pi} \right] \begin{cases} (q-1)k_{\mathrm{min}}^{q-1}, & \text{for } q > 1; \\ [\ln(k_{\mathrm{max}}/k_{\mathrm{min}})]^{-1}, & \text{for } q = 1; \\ (1-q)k_{\mathrm{max}}^{q-1}, & \text{for } q < 1; \end{cases} \tag{2}$$

where $\mathcal{E}_{\mathrm{tot}}$ is the total turbulence energy density.

Ions in a turbulent plasma can gain energy by interacting with the waves with diffusion coefficients D_{pp}, $D_{\mu p}$, and $D_{\mu\mu}$, where p is the momentum of the particles, and lose energy via Coulomb collisions with electrons and protons in the thermal background. As a result the particles diffuse in both real and momentum space. The spatial diffusion can be approximated with an escape term with a time scale T_{esc}. Because the Coulomb scattering rate at low energies and the pitch angle scattering rate $D_{\mu\mu}$ at high energies are larger than the acceleration rate (except for highly magnetized plasmas with $\alpha \ll 0.02$), the particle distribution is nearly isotropic over all energies. The energy diffusion rate $\gamma(\mu, p) = \tau_{\mathrm{ac}}^{-1}(\mu, p) = (D_{pp} - D_{\mu p}/D_{\mu\mu})/p^2$ (see Schlickeiser 1989; Dung & Petrosian 1994). As stressed in PL04, when the interaction is dominated by one of the resonant modes, this rate becomes negligibly small and the particle acceleration is suppressed. In PL04, we showed that such a suppression occurs for low energy protons but not for electrons. As mentioned above at low energies the ^{4}He interaction is dominated by one mode resulting in a low acceleration rate relative to ^{3}He. For isotropic pitch angle distribution, the particle distribution integrated over the acceleration region, $N(\varepsilon)$, as a function of the total (not per nucleon) kinetic energy ε, satisfies the well known diffusion-convection equation:

$$\frac{\partial N}{\partial t} = \frac{\partial^2}{\partial \varepsilon^2}(D_{\varepsilon\varepsilon}N) + \frac{\partial}{\partial \varepsilon}[(\dot{\varepsilon}_{\mathrm{L}} - A(\varepsilon))N] - \frac{N}{T_{\mathrm{esc}}} + Q, \tag{3}$$

where $D_{\varepsilon\varepsilon} = \varepsilon^2 < \gamma(\mu, p) > \sim \varepsilon A(\varepsilon)$ is the pitch angle averaged diffusion rate, Q is a source term, and the loss rate $\dot{\varepsilon}_{\mathrm{L}}$ is given in PL04.

Figure 2 shows the relevant time scales for a model with $L = 10^{10}$ cm, $B_0 = 500$ Gauss, $n_{\mathrm{e}} = 5 \times 10^9$ cm^{-3} and temperature $T = 0.2$ keV. The turbulence spectral index $q = 1$, $\tau_{\mathrm{p}}^{-1} = 3$ s^{-1} and $\alpha = 0.45$. The acceleration and loss times are defined as: $\tau_{\mathrm{a}} = \varepsilon/A(\varepsilon)$, $\tau_{\mathrm{loss}} = \varepsilon/\dot{\varepsilon}_{\mathrm{L}}$. Depending on L, τ_{p} and ε, either the transit time $\tau_{\mathrm{tr}} = (L/\sqrt{2}\beta c)$ or the diffusion time $\tau_{\mathrm{dis}} = 2\tau_{\mathrm{tr}}^2/\tau_{\mathrm{sc}}$ can dominate the escaping process, where τ_{sc} is the scattering time including both wave-particle scatterings and particle-particle collisions. We define $T_{\mathrm{esc}} = (L/\sqrt{2}\beta c)(1 + \sqrt{2}L/\beta c\tau_{\mathrm{sc}})$, which incorporates both processes of escape.

There are several features in these times, which require particular attention:

First, all the time scales are energy dependent and the acceleration times have complicated forms, in contrast to the often used simplified acceleration by pure Alfvén turbulence and/or with energy independent escape time. This affects the spectral shapes significantly.

Second, the typical time scale varies from less than one second to hundreds of seconds with different processes dominating at different energies.

Third, the acceleration times for ^{4}He and ^{3}He are quite different due to interaction with different waves, while their escape and loss times are similar because these times are dominated by Coulomb collisions and wave-particle scatterings ($\propto < D_{\mu\mu} >$).

Fourth, the acceleration time of ^{3}He is shorter than the Coulomb loss time below a few hundreds of keV nucleon^{-1}. Consequently, for a background plasma of a few million Kelvin almost all the injected ^{3}He can be accelerated to high energies (a few MeV nucleon^{-1}). Above this energy the escape time becomes shorter than the acceleration time and the acceleration is quenched.

Fifth, ^{4}He acceleration time increases sharply with the decrease of energy near 100 keV nucleon^{-1}. This is because at lower energies the wave-particle interaction is dominated by one of the resonant modes. ^{4}He acceleration time starts to decrease with energy near 50 keV nucleon^{-1} where the two resonant waves have comparable wavenumber (Figure 1). Because the acceleration time is longer than the loss time at low energies, for an injection plasma with a temperature less than $\sim 10^8$ K, only a small fraction of ^{4}He in the Maxwellian tail can be accelerated to very high energies. The rest is heated up into a quasi-thermal distribution.

Sixth, the acceleration time of ^{4}He is shorter than that of ^{3}He above ~ 100 keV nucleon^{-1}, so that the ^{4}He acceleration becomes more efficient at these energies.

3. Application to SEPs

Because the duration of SEPs are much longer than the characteristic time scales discussed in the previous section, we will assume that the system reaches a steady state. One can then ignore the time derivative term in equation (3) and solve this equation for the escaping flux $f = N/T_{\rm esc}$, which can be directly compared with the observed fluences.

Figure 3 shows our model fit to the spectra of an SEP event on January 6, 2000, the event with the largest ^{3}He enrichment (Mason et al. 2000). The data are obtained by carefully subtracting the background and avoiding contaminations from nearby events. For the model

spectra, we assume that the injected plasma has a coronal abundance, i.e. the abundance of ^{4}He is two thousand times higher than that of ^{3}He. The model parameters are the same as those in Figure 2. The temperature of 0.2 keV is a typical value for impulsive SEP events (Reames et al. 1994). Because the acceleration region is connected to open magnetic field lines probably above the flaring coronal loops, a size of $L = 10^{10}$cm seems quite reasonable. The magnetic field and gas density are also characteristic of an upper coronal reconnection region. The turbulence parameters q and $\tau_{\rm p}$ are free model parameters.

The model not only accounts for the enrichment of ^{3}He, but also gives a reasonable fit to the spectra. Because at low energies the acceleration time of ^{3}He is shorter than any other times, almost all of the injected ^{3}He ions are accelerated to a few hundreds of keV nucleon^{-1}, where $\tau_{\rm a}$ becomes longer than the loss and escape time, resulting in a sharp cutoff. The ^{4}He acceleration time, because of the barrier mentioned above, is much longer than its loss time below a few keV nucleon^{-1}. This suppresses the ^{4}He acceleration so that most of the injected ^{4}He ions remain near the injection energy and form a quasi-thermal component. However, even when $A(\varepsilon) \leq \dot{\varepsilon}_{\rm L}$ and the direct acceleration is difficult, some ^{4}He ions can still diffuse to high energies due to the first term on the right hand side of equation (3). Consequently, we expect a nonthermal tail in addition to the quasi-thermal component. This tail is cut off at ~ 10 MeV nucleon^{-1} (Fig. 3), when the escape time becomes much shorter than the acceleration time (Fig. 2). The acceleration barrier extends to ~ 100 keV nucleon^{-1}, most of the ^{4}He ions diffuse to higher energies are stopped below this energy. About 10% of the particles can be accelerated to even higher energies and produce the observed high energy spectrum with some spectral features in this energy range. However, a more realistic model, including acceleration by other wave modes, is expected to produce smoother spectra.

The above behaviors depend on six model parameters, which are shown in Figure 2 (note that α is given by $n_{\rm e}$ and B_0 via eq.[1]). Figure 4 shows how the spectra change with two of these parameters: $\tau_{\rm p}^{-1}$ (or the energy density of the turbulence) and the injection temperature T. Because of the acceleration barrier at low energies, the acceleration of ^{4}He is very sensitive to T. In the figure, we adjust $\tau_{\rm p}$ in order to make the fluence of ^{4}He and ^{3}He comparable at a few hundred keV per nucleon. As evident, ^{3}He spectrum peaks at a higher energy with the increase of the intensity of the turbulence and the ^{3}He enrichment also changes significantly. This can explain the variation of the ^{3}He spectral peak and its enrichment in class 2 SEPs (Mason et al. 2000; Mason, Mazur & Dwyer 2002).

4. Summary and Discussion

In the paper, we have shown that the observed ^{3}He and ^{4}He spectra in some impulsive SEPs can be produced via SA by PWT propagating parallel to magnetic field lines. In the model, the particles are injected from a thermal background. Because the interaction of low energy ^{4}He is dominated by one of the resonant wave modes, an acceleration barrier forms, giving rise to a prominent quasi-thermal component in the steady state particle spectrum. This is not true for ^{3}He ions, however, which can be efficiently accelerated by two waves in the PC branch, from very low energies to $\sim$ MeV nucleon^{-1}, where they escape quickly from the acceleration site, producing a sharp spectral cutoff. This explains the ^{3}He enrichment and its varied spectrum seen in class 2 SEPs, which have relatively short rise-time and are more likely associated with the impulsive phase particle acceleration directly. Class 1 events have less ^{3}He enrichment and similar spectra for most ions, indicating a different acceleration process (Mason et al. 2000). The feasibility of producing such events by shocks or turbulence with a different spectrum than that of the present model will be investigated in the future.

Because the ^{4}He acceleration time is shorter than that of ^{3}He at higher energies and their loss and escape times are comparable, the model predicts a decrease of the ^{3}He to ^{4}He ratio with energy beyond ~ 1 MeV nucleon^{-1}, which is consistent with observations (Mason et al. 2002; Reames et al. 1997; Möbius et al. 1982; Möbius et al. 1980; Hsieh & Simpson 1970). Spectral information at higher energies is critical in testing this model prediction. *We emphasize here that a special injection mechanism is not required to explain the observations.* However, a second-phase shock acceleration (Van Hollebeke, McDonald & Meyer 1990) can modify the ion spectra and may explain events where the high energy spectral indices of ^{3}He and ^{4}He are similar (Serlemitsos & Balasubrahmanyan 1975; Reames et al. 1997).

The model can also be applied to acceleration of heavy-ions. In this case, the acceleration is dominated by resonant interaction with waves in the HeC branch and ions with low charge to mass ratio are accelerated more efficiently, which may explain the increase of ion enrichment with the increase of their charge to mass ratio (Mason et al. 1986). Because ^{3}He acceleration is dominated by interaction with the PC branch, which may be decoupled from the HeC branch, the model may also explain the lack of quantitative correlation of the enrichment of ^{3}He and heavy-ions (Mason et al. 1986). We will investigate these aspects in future work.

The primary uncertainties of the model are associated with the turbulence generation mechanism and the subsequent cascade and dissipation processes. We start the investigation with a power law spectrum of the wavenumber for the turbulence, which can be characterized by the turbulence energy density and the spectral index. The acceleration of particles by obliquely propagating waves and turbulence with complex spectral shapes may give quanti-

tatively different results. However, the idea of an efficient depletion of low energy ^{3}He from the source region to high energies to produce the observed enhancement seems well founded.

REFERENCES

Dung, R., & Petrosian, V. 1994, ApJ, 421, 550

Fisk, L. A. 1978, ApJ, 224, 1048

Hamilton, R. J., & Petrosian, V. 1992, ApJ, 398, 350

Hsieh, K. C., & Simpson, J. A. 1970, ApJ, 162, L191

Hua, X. M., Ramaty, R., & Lingenfelter, R. E. 1989, ApJ, 341, 516

Hurford, G. J., Mewaldt, R. A., Stone, E. C., & Vogt, R. E. 1975, ApJ, 201, L95

Mason, G. M., Dwyer, J. R., & Mazur, J. E. 2000, ApJ, 545, L57

Mason, G. M., Mazur, J. E., & Dwyer, J. R. 2002, ApJ, 565, L51

Mason, G. M., Reames, D. V., Klecker, B., Hovestadt, D., & von Rosenvinge, T. T. 1986, ApJ, 303, 849

Mason et al. 2002, ApJ, 574, 1039

Mazur, J. E., Mason, G. M., & Klecker, B. 1995, ApJ, 448, L53

Miller, J. A. 2003, Multi-Wavelength Observations of Coronal Structure and Dynamics eds. Petrus C.H. et al. (COSPAR Colloquia Series Vol. 13), 387

Miller, J. A., & Ramaty, D. A. 1987, Sol.Phys., 113, 195

Miller, J. A., & Viñas, A. F. 1993, ApJ, 412, 386

Möbius, E., Hovestadt, D., Klecker, B., & Gloeckler, G. 1980, ApJ, 238, 768

Möbius, E., Scholer, M., Hovestadt, D., Klecker, B., & Gloeckler, G. 1982, ApJ, 259, 397

Paesold, G., Kallenbach, R., & Benz, A. O. 2003, ApJ, 582, 495

Petrosian, V., & Donaghy, T. Q. 1999, ApJ, 527, 945

Park, B. T., Petrosian, V., & Schwartz, R. A. 1997, ApJ, 489, 358

Petrosian, V., & Liu, S. 2004, ApJ, (submitted); preprint at <astro-ph/0401585>

Ramaty, R. 1979, in Particle Acceleration Mechanisms in Astrophysics, eds. J. Arons, C. Max, & C. McKee (New York: AIP) 135

Reames, D. V., Barbier, L. M., von Rosenvinge, T. T., Mason, G. M., Mazur, J. E., & Dwyer, J. R. 1997, ApJ, 483, 515

Reames, D. V., Meyer, J. P., & von Rosenvinge, T. T. 1994, ApJS, 90, 649

Reames, D. V., von Rosenvinge, T. T., & Lin, R. P. 1985, ApJ, 292, 716

Schlickeiser, R. 1989, ApJ, 336, 243

Serlemitsos, A. T., & Balasubrahmanyan, V. K. 1975, ApJ, 198, 195

Steinacker, J., Meyer, J. P., Steinacker, A., & Reames, D. V. 1997, ApJ, 476, 403

Sakurai, K. 1974, Ap&SS, 28, 375

Temerin, M., & Roth, I. 1992, ApJ, 391, L105

Van Hollebeke, M. A. I., McDonald, F. B., & Meyer, J. P. 1990, ApJ, 73, 285

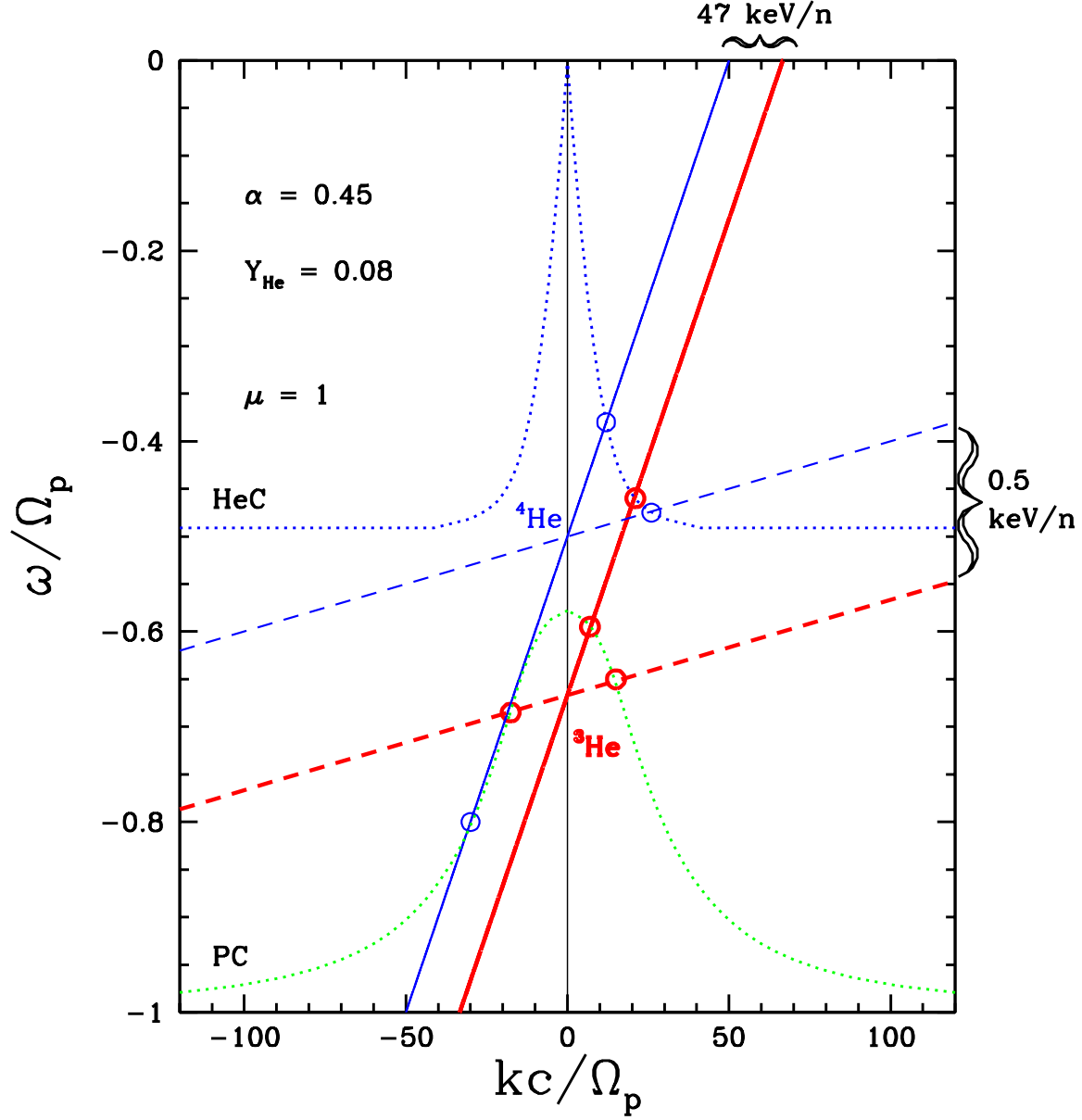Zhang, T. X. 1995, ApJ, 449, 916

Zhang, T. X. 1999, ApJ, 518, 954

Fig. 1.— *Dotted curves:* dispersion relation of PC and HeC left hand polarized waves parallel to the large scale magnetic field. *Solid lines:* resonant condition for 47 keV/nucleon ^{3}He (*thick*) and ^{4}He (*thin*). *Dashed lines:* resonant condition for 0.5 keV/nucleon. Circles designate the resonant points.
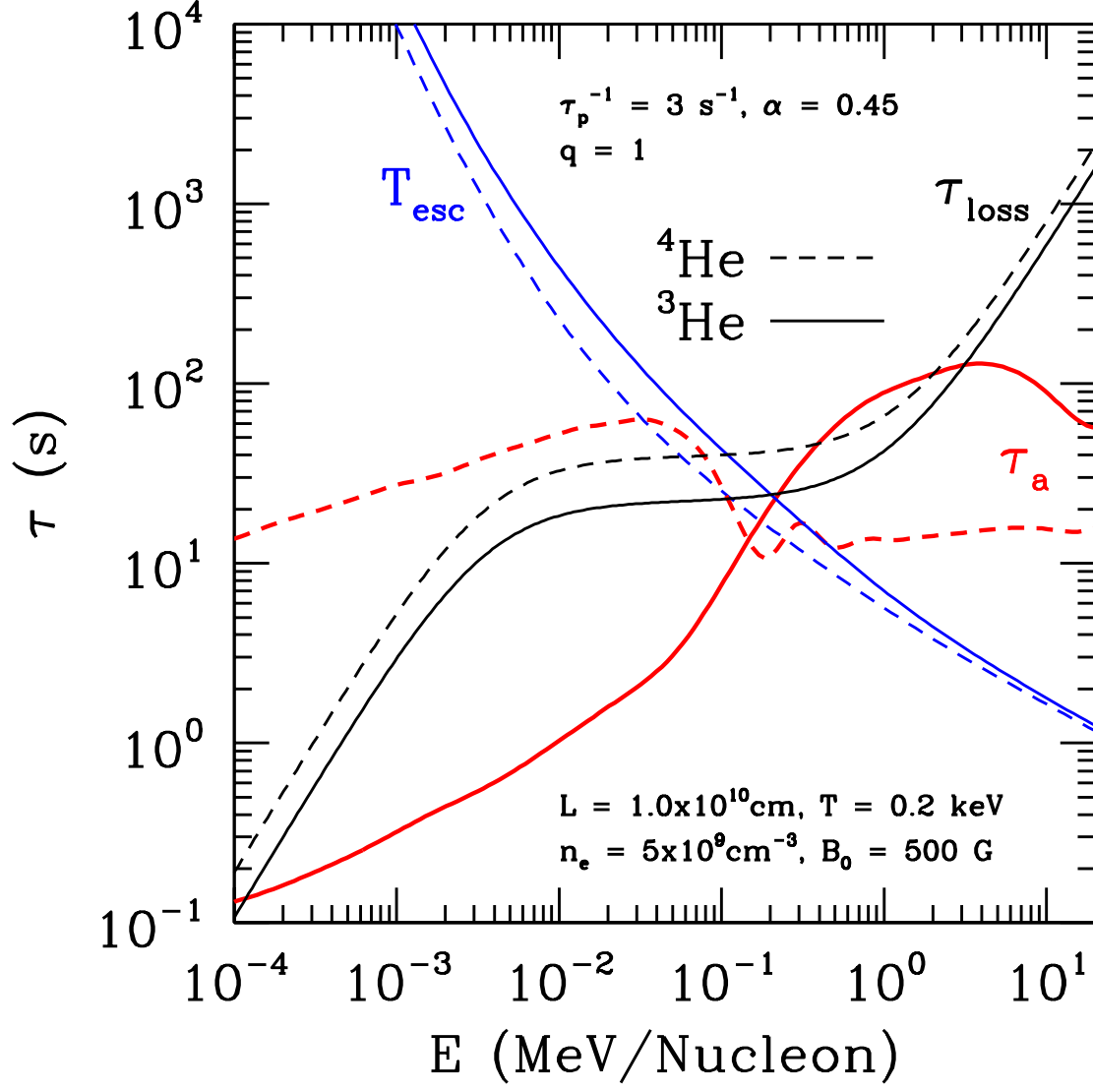
Fig. 2.— Time scales of a SA acceleration model. The model parameters are indicated in the figure. *Solid:* ³He, *dashed:* ⁴He. The thicker curves indicate the acceleration times. See text for details.
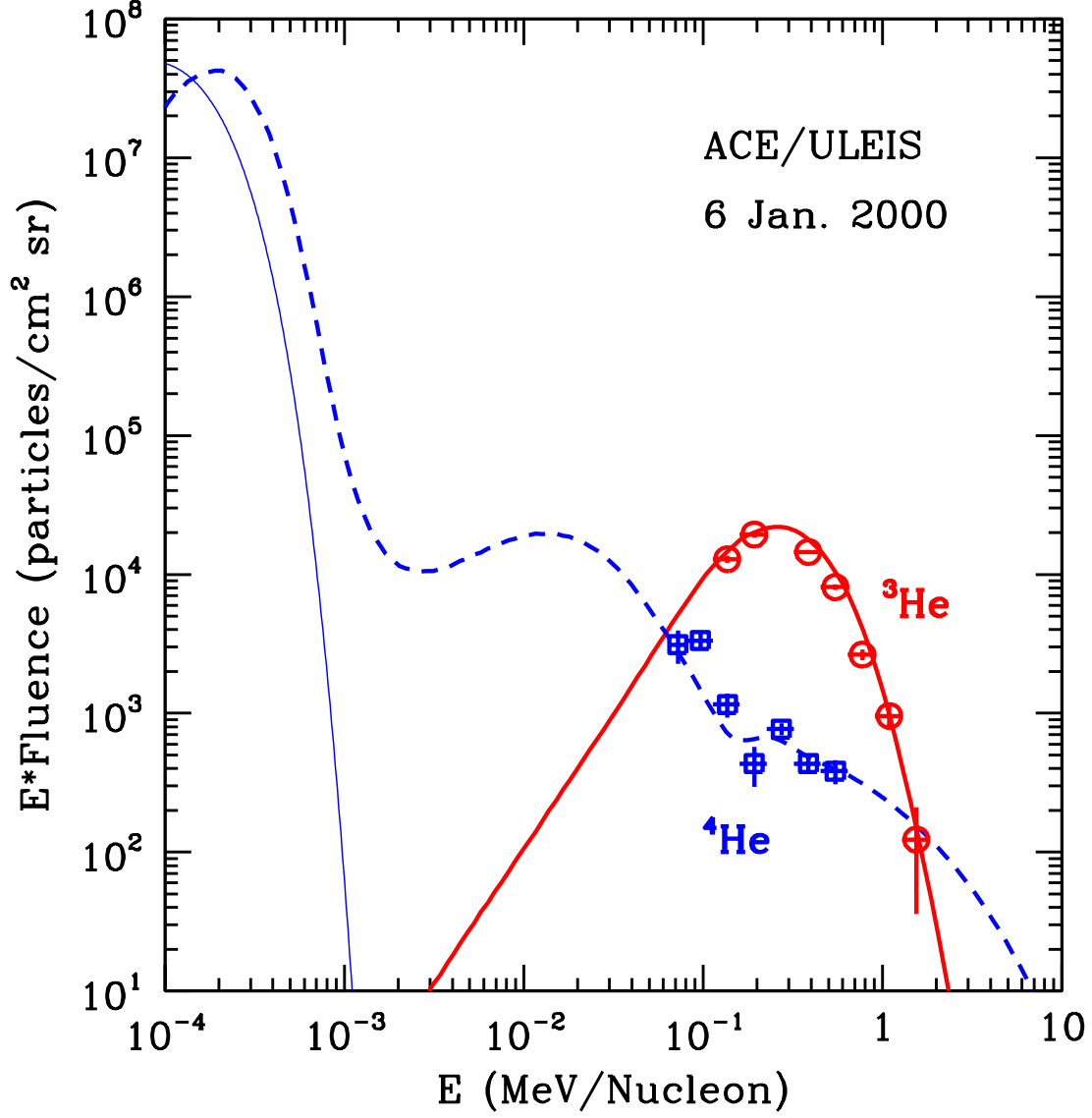
Fig. 3.— Model fit to the spectra of the SEP on Jan. 6, 2000. The thick solid curve is for ^{3}He and the dashed curve is for ^{4}He. The injected particles have a temperature of $T = 0.2$ keV and the corresponding distribution of ^{4}He is indicated by the thin solid curve with arbitrary normalization. All other model parameters are shown in Figure 2.
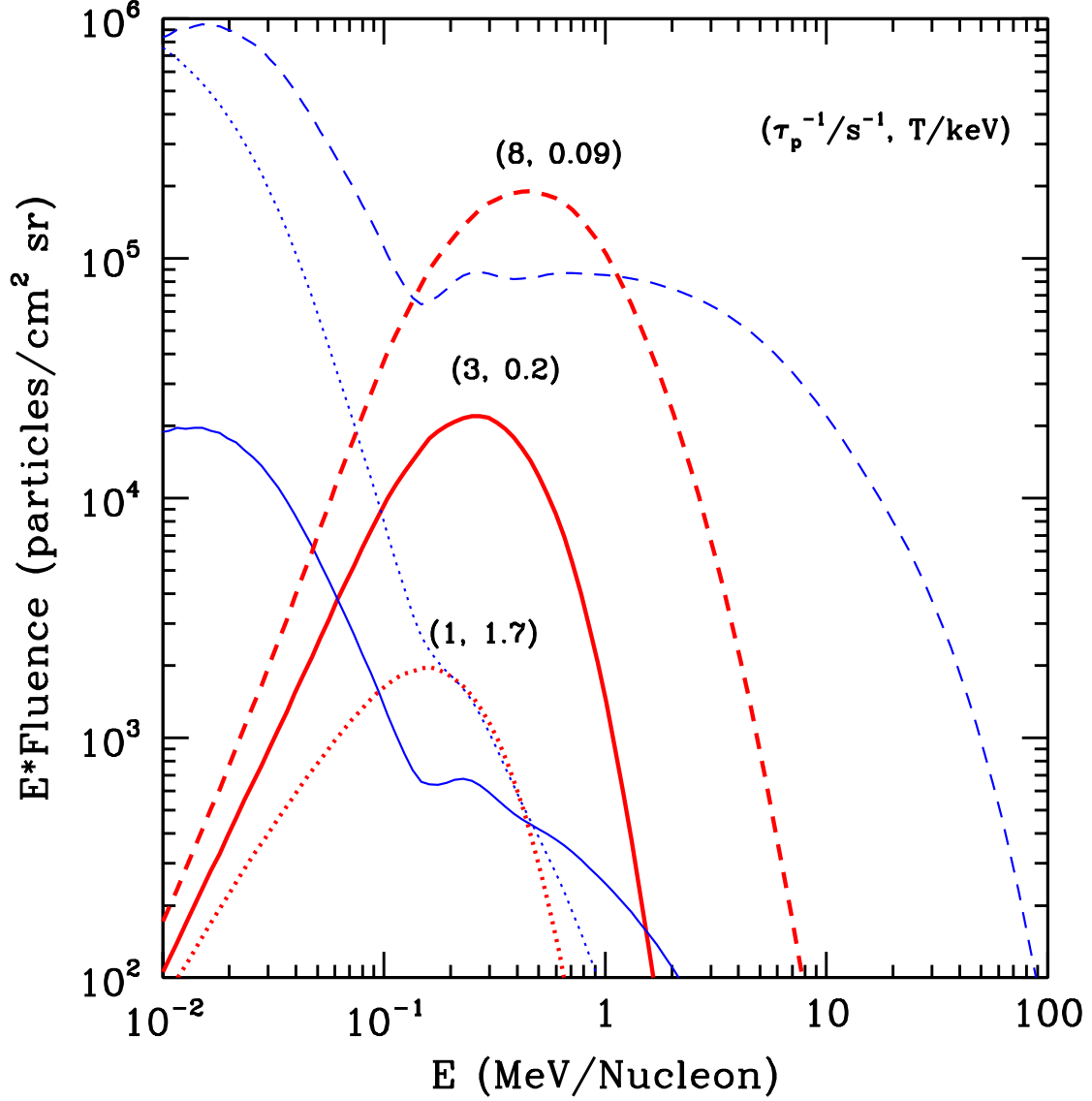
Fig. 4.— Dependence of the ^{3}He (thick curves) and ^{4}He (thin curves) spectrum on τ_p and T. The dotted, solid, and dashed curves are for $\tau_p^{-1} = 1$, 3, and 8 s^{-1} and $T = 1.7$, 0.2, and 0.09 keV, respectively. The dotted (dashed) curves are shifted up (down) by decade. All other model parameters remains the same as those in Figure 2.